Goldstone Modes and Low-Frequency Dynamics of Incommensurate Chromium Alloys

R. S. Fishman
Solid State Division, Oak Ridge National Laboratory, P.O. Box 2008, Oak Ridge, Tennessee 37831-6032

S. H. Liu
Physics Department, University of California, San Diego, California 92093
(Received 18 October 1995)

This Letter reports the first solution for the low-energy spin excitations about the incommensurate spin-density-wave (SDW) state of pure Cr and Cr alloys. The Goldstone modes evolving from the magnetic satellites consist of transverse spin-wave modes and longitudinal phason modes, which are associated with the rotational and translational symmetries of the SDW state, respectively. The phason modes bend toward the zone boundary H between the satellites and produce the recently observed 60 meV peak in the longitudinal cross section at H. We also report a new class of collective excitation which is associated with oscillations of the SDW wave vector.

PACS numbers: 75.30.Fv, 75.30.Ds, 75.40.Gb

Unlike the local magnetic moments of rare earth metals, the spin-density wave (SDW) of chromium and its dilute alloys consists of bound electron-hole pairs [1]. Since the ordered magnetic moments may fluctuate in magnitude, the spin excitations about the SDW state are more complex than the spin-wave (SW) modes in conventional antiferromagnets. Although pure Cr and many of its alloys order in an incommensurate (I) phase [1], in which the SDW is incommensurate with the bcc lattice, all previous theoretical work on the spin dynamics is itinerant antiferromagnets [2–9] has employed a simplistic band structure only appropriate in the commensurate (C) phase. But recent experiments [10–13] indicate that theoretical results for the C phase do not extrapolate well to the I phase. In this Letter, we present the first detailed analysis of the Goldstone modes of an I transition metal antiferromagnet.

Chromium metal is susceptible to the formation of a SDW because of the almost perfectly nested electron a and slightly larger hole b Fermi surfaces [1], both of which are roughly octahedral in shape. For pure Cr, the mismatch ∂ of the nesting wave vectors $Q_\pm = (G/2)(1 \pm \partial)$ on either side of $G/2 = 2\pi/a$ is about 0.036. When Cr is doped with either Mn or Fe, the electron surface grows and this mismatch decreases; doping with V enlarges the hole surface and increases ∂. As first envisioned by Lomer [14], the Coulomb attraction $V > 0$ between electrons and holes produces a SDW consisting of spin-triplet electron-hole pairs with order parameter g.

As shown in Fig. 1(a), the actual wave vectors of the SDW are given by $Q'_\pm = (G/2)(1 \pm \partial')$ where $0 \le \partial' < \partial$. The short-dashed lines in Fig. 1(b) denote the paramagnetic energies near an octahedral face of the Fermi surface with normal $\hat{n}$ and $k_z > 0$; the long-dashed horizontal line is the chemical potential. In this figure, $z = v_F(\vec{k} \cdot \hat{n} - k_F)$ specifies the momentum difference from an octahedral face of the Fermi surface, $z_0 = 4\pi\partial v_F/\sqrt{3}\,a$ measures the energy mismatch between the electron and hole surfaces, and $\kappa = z_0\partial'/2\partial$ controls the incommensurability of the SDW. Here, k_F is the shortest Fermi wave vector from the zone center Γ to the zone boundary H. For pure Cr, $z_0 \approx 375$ meV and $\kappa \approx 150$ meV.

Translating the hole Fermi surface by $Q'_\pm$ rather than $Q_\pm$ worsens the nesting on one side of the Fermi surface (so that $z_0/2 - \kappa > 0$) while improving it on the other side ($z_0/2 + \kappa < z_0$). The SDW wave vectors $Q'_\pm$ are then determined by the competition between the nesting free energies on each side of the electron and hole Fermi surfaces [15]. Doping with more than [1] 0.3% Mn or 2.4% Fe stabilizes the CSDW state with $\partial' = 0$. Pure Cr

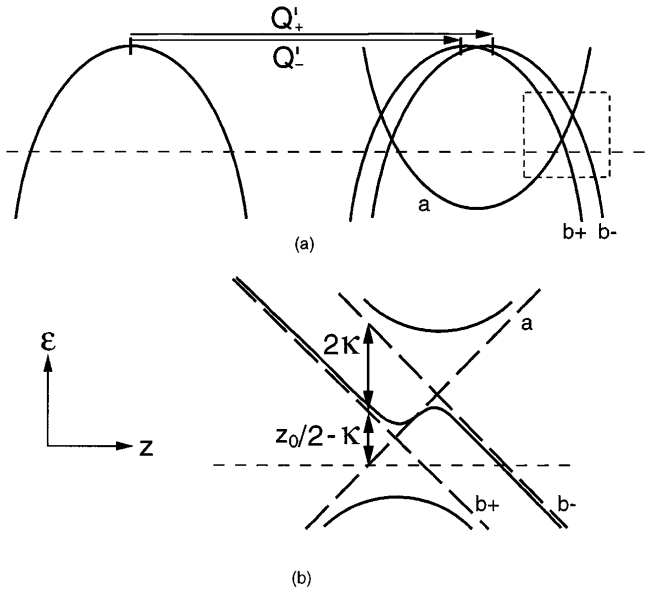

FIG. 1. (a) The electron (a) and hole (b) energies translated by the SDW wave vectors $Q'_\pm$. In (b), we expand the boxed region near the Fermi energy for the quasiparticle energies above (short dashed) and below (solid) the Néel temperature. In both (a) and (b), the chemical potential is denoted by a horizontal dashed line.

 0031-9007/96/76(13)/2398(4)$10.00

and CrV alloys are in an ISDW state with $\partial' > 0$. The three domains for the SDW wave vectors $\vec{Q}'_{\pm}$ correspond to the possible directions for the nesting wave vectors $\vec{Q}_{\pm}$. In this paper, we choose the SDW wave vectors to lie along the z axis.

The spin associated with each ISDW at site $\vec{R}$ is

$$\vec{S}_{\pm}(\vec{R}) = \hat{m}\alpha_s g \exp\{i(\vec{Q}_{\pm} \cdot \vec{R} + \phi_{\pm})\}, \quad (1)$$

where $\alpha_s = -2\hbar/V$ and the phase constants $\phi_{\pm}$ may be different for the two ISDW's. Then the total spin at $\vec{R}$ is given by $\vec{S}(\vec{R}) = \vec{S}_{+}(\vec{R}) + \vec{S}_{-}(\vec{R})$. The low-frequency Goldstone modes of I Cr alloys are associated with the invariance of the free energy under translations and rotations of the ISDW state in Eq. (1). While transverse SW modes are associated with the free energy's rotational invariance, longitudinal phason modes are associated with its translational invariance. Both sets of modes evolve from the SDW ordering wave vectors $\vec{Q}'_{\pm}$. Another unexpected class of collective modes is associated with oscillations of the SDW wave vectors $\vec{Q}'_{\pm}$. We call these new excitations "wavons."

We have analyzed the excitations about the two ISDW states of Eq. (1) using the random-phase approximation (RPA). While it remains the simplest formalism to study the spin dynamics of any magnetic system, the RPA was never applied to the full ISDW state for the following reason. The spin dynamics of an itinerant antiferromagnet are driven by quasiparticle transitions. So to realistically study the spin dynamics of I alloys, three bands must be used for the quasiparticle energies: one for the electrons a and two for the holes $b\pm$. This greatly complicates the formulation of the RPA and makes low-frequency or wave vector expansions unreliable. Our results were obtained after a careful formulation [16] of the RPA within the three-band model for all temperatures and mismatch energies without any further approximations.

As plotted in the solid lines of Fig. 1(b) for $k_z > 0$, the electron and hole energies hybridize below the Néel temperature. At $T = 0$, $ab+$ pairs and $b-$ holes completely fill the available states below the chemical potential. In contrast to the simpler two-band model developed by Fedders and Martin [2], the three-band model by Young and Sokoloff [17] allows quasiparticle transitions between $ab+$ and $ab-$ condensates of electron-hole pairs.

For simplicity, we only consider spin fluctuations with wave vector $\vec{q}$ along the $\hat{z}$ direction. Then spin fluctuations with frequency ω and momentum $\vec{q}$ correspond to quasiparticle transitions with energy change ω and momentum difference specified by $\Delta z = v_F \vec{q} \cdot \hat{n} = v_F q \,\mathrm{sgn}(k_z)/\sqrt{3}$. This factor of $\sqrt{3}$ eventually finds its way into the SW mode velocity $c = v_F/\sqrt{3}$.

The ISDW state has two ordering wave vectors, so its spin susceptibility contains two sets of contributions centered around each SDW wave vector:

$$\chi_t(\vec{q},\omega) = 2[\chi_{-}(\vec{q} - \vec{w},\omega) + \chi_{-}(-\vec{q} - \vec{w},\omega)], \quad (2)$$

$$\chi_l(\vec{q},\omega) = \chi_{+}(\vec{q} - \vec{w},\omega) + \chi_{+}(-\vec{q} - \vec{w},\omega), \quad (3)$$

$$\chi_{\pm}(\vec{q},\omega) = -2/V + [t_{1\pm}(\vec{q},\omega) + it_{2\pm}(\vec{q},\omega)]^{-1}, \quad (4)$$

where $\vec{w} = (2\pi\partial'/a)\hat{z}$ and $V > 0$ is the attractive Coulomb interaction between the electrons and holes. In Eqs. (2) and (3), the wave vector $\vec{q}$ is measured from $(G/2)\hat{z}$. Hence, the crystal momentum $\vec{p}$ associated with fluctuations of wave vector $\vec{q}$ is $\vec{p} = \vec{q} + (G/2)\hat{z}$. In Eq. (4), $t_{1\pm}$ and $t_{2\pm}$ are real functions of $\vec{q}$ and ω which are given elsewhere [15]. Here we shall be primarily concerned with their analytic properties. The transverse and longitudinal cross sections are proportional to the imaginary parts of $\chi_t(\vec{q},\omega)$ and $\chi_l(\vec{q},\omega)$.

While the first terms in Eqs. (2) and (3) have zero-frequency poles at the satellite wave vector $\vec{Q}'_{+}$, the reflected terms with $\vec{q} \to -\vec{q}$ produce the satellite at $\vec{Q}'_{-}$. Above the Néel temperature, $t_{1+} = t_{1-}$ and $t_{2+} = t_{2-}$. Consequently, $\chi_t = 2\chi_l$ and the spin fluctuations are isotropic. Below the Néel temperature, the collective modes are given by the zeros of the denominator $t_{1\pm} + it_{2\pm}$. By summing the contributions from each SDW, Eqs. (2) and (3) distinguish the collective modes about one SDW from the collective modes about the other. Hence, the collective modes about $\vec{Q}'_{\pm}$ are not affected by the spin excitations about $\vec{Q}'_{\mp}$.

A rich spectrum of collective excitations is produced by the complex quasiparticle energies of I Cr alloys. In this paper, we concentrate on the Goldstone modes which evolve from the SDW wave vectors and the new wavon modes mentioned above. At zero frequency, both the longitudinal and transverse susceptibilities have poles at $\vec{Q}'_{\pm}$ with $t_{1\pm}(0,0) = t_{2\pm}(0,0) = 0$. At nonzero frequencies, these poles develop into the transverse SW modes and the longitudinal phason modes. Other modes associated with the oscillation of the SDW amplitude $\alpha_s g$ in Eq. (1) are discussed in a more lengthy treatment [16].

The transverse SW modes have linear dispersion $\omega = c|q \pm w|$ with the same mode velocity $c = v_F/\sqrt{3} \approx 1500$ meV Å as in the C regime [8]. Because of the large size of this mode velocity, the splitting of each satellite into side peaks is difficult to observe experimentally. Measurements in the C phase [18,19], however, indicate that the SW velocity is about 30% smaller than predicted. But as discussed in Ref. [16], the effective SW velocity may be shifted by the background of incoherent excitations. Although the mode velocity c is independent of temperature, the strength s_t of each SW mode, defined as the integral over cq of the SW delta function in $\mathrm{Im}\chi_t(q,\omega)$, is proportional [16] to g^2/ω. So the SW strength vanishes as T approaches T_N and decreases with increasing frequency.

By contrast, Sato and Maki [4] found that within a two-band model the SW mode velocity is proportional to g and vanishes as $T \to T_N$. A similar result was found by others [20,21] starting with a phenomenological

free energy of local spins [22] obeying the canonical commutation rules near T_N. We believe that neither of these approaches is appropriate for incommensurate itinerant antiferromagnets.

Phason modes are produced by the dynamics of the phases $\phi_\pm(\vec{R},t)$ in Eq. (1). Supposing ϕ_0 to be the equilibrium phase and setting $\delta\phi(\vec{R},t) = \phi_\pm(\vec{R},t) - \phi_0$, the change in local spin is given by

$$\delta\vec{S}_\pm(\vec{R},t) = \hat{m} i \alpha_s g \delta\phi(\vec{R},t) \exp\{i(\vec{Q}'_\pm \cdot \vec{R} + \phi_0)\}, \tag{5}$$

which is parallel to the spin polarization direction $\hat{m}$. Hence, phasons are longitudinal excitations which evolve from the ISDW wave vectors at $\vec{Q}'_\pm$. In the C phase, shifting the phase of the CSDW will change the magnitude of the spin on each sublattice. Hence, phason modes do not appear [9] in the C dynamics.

Since the pole in the longitudinal susceptibility is damped at nonzero frequencies so that $t_{2+}(\vec{q},\omega) < 0$, the dispersion of the phason modes is determined by the condition $t_{1+}(\vec{q},\omega) = 0$. For small frequencies, the phasons evolve linearly with mode velocity $c_{\rm ph} < c$. As shown in Fig. 2, the phason mode velocity approaches the SW velocity as $T \to T_N$. The phason velocity also increases with the incommensurability energy z_0, which grows linearly with the V concentration in CrV alloys.

The phason modes have often been mistaken for SW's because they also evolve from the satellite wave vectors and have velocities of order v_F. In the longitudinally polarized SDW state below 120 K for pure Cr, pinning energies [10] of unknown origin constrain the spin fluctuations parallel to $\hat{m}$ and $\vec{Q}'_\pm$. So the low-frequency, longitudinal excitations observed by Burke *et al.* [10] were actually phason modes. By contrast, the low-frequency Fincher-Burke excitations [10,21] with velocities of order $v_F/50$ are probably unrelated to the phason modes. We are currently investigating the possibility that these low-frequency modes are actually produced by the coupling between the spin and lattice dynamics, mediated by an associated charge-density wave.

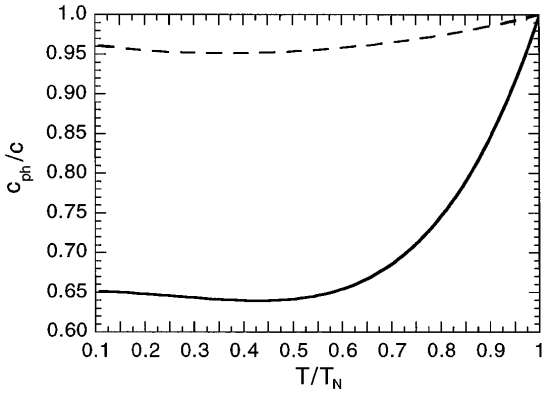

FIG. 2. The phason mode velocity $c_{\rm ph}$ normalized by the SW velocity vs T/T_N for $z_0/T_N^* = 4.7$ (solid) or 7.0 (dashed).

In Fig. 3, we graph the SW and phason modes evolving from the two ISDW satellites at $T/T_N = 0.5$. The energy scale $T_N^* \approx 80$ meV is the Néel temperature of perfectly nested Cr with $\partial' = \partial = 0$. Then the value $z_0 = 4.7T_N^* \approx 375$ meV used in Figs. 2 and 3 should roughly correspond to pure Cr. For these parameters, the two satellites lie at $cq = \pm cw = \pm\kappa \approx \pm 1.903 T_N^*$. As shown, the phason modes evolve linearly up to a frequency of about $0.4T_N^* \approx 32$ meV. Above $0.75T_N^* \approx 60$ meV, the phason modes become overdamped and disappear. At this frequency, the inner phasons smoothly join another damped longitudinal excitation discussed in Ref. [16]. The intersection of the inner phason modes with $q = 0$ (reciprocal lattice point H) was very recently observed by Fukuda *et al.* [13] as a 60 meV peak in the $G/2$ cross section. Although the peak will broaden with increasing temperature, the peak frequency should change very little in the range $0 < T/T_N < 0.7$, where the phason mode velocity is almost constant. The inner phasons also bend the SW cones toward H, as first observed by Fincher, Shirane, and Werner [23].

An unexpected class of collective excitations called wavons is associated with oscillations of the ordering wave vectors $\vec{Q}'_\pm$ about their equilibrium values. If the wave vector fluctuation $\delta\vec{Q}(\vec{R},t) = \vec{Q}(\vec{R},t) - \vec{Q}'_\pm$ coincides with the variation in the polarization direction from $\hat{m}$ to $\hat{m}'(\vec{R},t) = \hat{m} + \delta\vec{m}(\vec{R},t)$, then the change in spin may be written

$$\delta\vec{S}_\pm(\vec{R},t) = \alpha_s g([\hat{m} + \delta\vec{m}(\vec{R},t)] \exp\{i\delta\vec{Q}(\vec{R},t) \cdot \vec{R}\} - \hat{m}) \times \exp\{i(\vec{Q}_\pm \cdot \vec{R} + \phi_0)\}, \tag{6}$$

which contains both transverse and longitudinal components. Transverse wavons involve the coherent oscillation of both the spin polarization direction and the SDW wave vector. This combination of infinitesimals is possible because Eq. (6) cannot be linearized in $\delta\vec{Q}$. Wavons transform into SW's as $\delta Q/\delta m \to 0$. So as shown

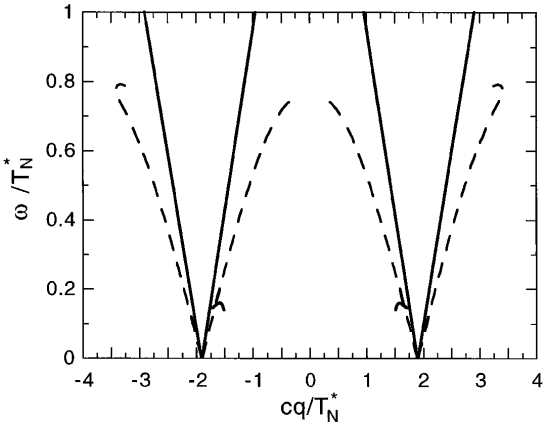

FIG. 3. Normalized frequency ω/T_N^* vs wave vector cq/T_N^* for the transverse SW (solid) and longitudinal phason (dashed) modes with $z_0/T_N^* = 4.7$ and $T/T_N = 0.5$. Also shown are wavon modes which terminate on the inner SW's.

in Fig. 3, degenerate transverse and longitudinal wavon modes terminate on the inner SW branches. An additional longitudinal wavon mode is located close to the third harmonic of the SDW [16].

The range of allowed wave vectors for the wavon modes is always less than the difference $Q_+ - Q'_+ = 2\pi(\partial - \partial')/a$ between the ordering and nesting wave vectors, which decreases with V doping. The wavons also disappear in the C limit $\partial' \to 0$. Recently, Endoh *et al.* [12] observed the wavon modes as a peak in the satellite cross sections between 15 and 20 meV, which is slightly smaller than our estimate of $0.28T_N^* \approx 22$ meV for $T/T_N = 0.2$. Our model predicts that this peak frequency should decrease as the temperature increases and vanish as $T \to T_N$.

It is interesting to compare the incommensurate spin dynamics of a transition metal antiferromagnet with the incommensurate dynamics of other systems. For a one-dimensional organic conductor [24], the ISDW wave vector $Q = 2k_F$ is fixed solely by a nesting criterion across the electron Fermi surface. So the nesting and ordering wave vectors coincide. Using a linear-response formalism in one dimension, Psaltakis [8] found that the phason mode velocity $c_{\rm ph}$ is equal to v_F at zero temperature. Since the SW velocity in one dimension also equals v_F, Psaltakis' result is consistent with our finding that $c_{\rm ph} \to c$ as $z_0 \to \infty$ and $Q'_\pm \to Q_\pm$. Psaltakis did not evaluate the phason mode dispersion for nonzero frequencies.

Wavon modes are not present in a one-dimensional organic conductor because the nesting and SDW wave vectors are identical. The wavon modes owe their existence to the unique physics of an I transition metal antiferromagnet, where the SDW wave vectors $Q'_\pm$ are fixed by the competition between the nesting free energies on the two sides of the electron and hole Fermi surfaces.

Phason modes of the charge density play an important role in structurally incommensurate systems [25]. Like SDW phasons, phasons of the charge-density wave (CDW) also evolve linearly for small frequencies and are damped for any nonzero frequency. The softening of a CDW phason, for example [26], in TTF-TCNQ, will induce a structural phase transition.

The predictions of our work on the incommensurate spin dynamics may easily be tested experimentally. With V doping, the phason velocity $c_{\rm ph}$ of CrV alloys increases and the phasons will intersect $q = 0$ at a higher energy; so at low temperatures, the 60 meV peak in the $G/2$ cross section should move to higher energies. On the other hand, the wavon mode frequency decreases as the difference between the nesting and SDW wave vectors becomes smaller; so the peak in the satellite cross section should shift downwards with V doping.

R. F. acknowledges support from the U.S. Department of Energy under Contract No. DE-FG06-94ER45519 and under Contract No. DE-AC0584OR21400 with Martin Marietta Energy Systems, Inc. S. L. thanks Professor L. Sham and Professor R. Dynes for their hospitality at UCSD. Useful conversations with J. Cooke, Y. Endoh, E. Fawcett, B. Sternlieb, and V. S. Viswanath are also gratefully acknowledged.

[1] For comprehensive reviews of Cr alloys, see E. Fawcett, Rev. Mod. Phys. **60**, 209 (1988) and E. Fawcett, H. L. Alberts, V. Yu Galkin, D. R. Noakes, and J. V. Yakhmi, Rev. Mod. Phys. **66**, 26 (1994).
[2] P. A. Fedders and P. C. Martin, Phys. Rev. **143**, 8245 (1966).
[3] S. H. Liu, Phys. Rev. B **2**, 2664 (1970).
[4] H. Sato and K. Maki, Int. J. Magn. **4**, 163 (1973); **6**, 183 (1974).
[5] M. B. Walker, Can. J. Phys. **54**, 1240 (1976).
[6] T. Wolfram and S. Elliatioglu, Phys. Rev. Lett. **44**, 1295 (1980).
[7] Y. Kurihara, J. Phys. Soc. Jpn. **51**, 2123 (1982).
[8] G. C. Psaltakis, Solid State Commun. **51**, 535 (1984).
[9] R. S. Fishman and S. H. Liu, Phys. Rev. B **50**, 4240 (1994).
[10] S. K. Burke, W. G. Stirling, K. R. A. Ziebeck, and J. G. Booth, Phys. Rev. Lett. **51**, 494 (1983).
[11] J. E. Lorenzo, B. J. Sternlieb, G. Shirane, and S. A. Werner, Phys. Rev. Lett. **72**, 1762 (1994).
[12] Y. Endoh, T. Fukuda, K. Yamada, and M. Takeda, J. Phys. Soc. Jpn. **63**, 3572 (1994).
[13] T. Fukuda, Y. Endoh, K. Yamada, M. Takeda, S. Itoh, M. Arai, and T. Otomo (to be published).
[14] W. M. Lomer, Proc. Phys. Soc. London **80**, 489 (1962).
[15] R. S. Fishman and S. H. Liu, Phys. Rev. B **48**, 3820 (1993).
[16] R. S. Fishman and S. H. Liu (unpublished).
[17] C. Y. Young and J. B. Sokoloff, J. Phys. F **4**, 1304 (1974).
[18] S. K. Sinha, S. H. Liu, L. D. Muhlestein, and N. Wakabayashi, Phys. Rev. Lett. **23**, 311 (1969); S. K. Sinha, G. R. Kline, C. Stassis, N. Chesser, and N. Wakabayashi, Phys. Rev. B **15**, 1415 (1977).
[19] J. Als-Nielsen, J. D. Axe, and G. Shirane, J. Appl. Phys. **42**, 1666 (1971).
[20] Yu. A. Izyumov and V. M. Laptev, Sov. Phys. JETP **61**, 95 (1985).
[21] X. Zhu and M. B. Walker, Phys. Rev. B **34**, 8064 (1986).
[22] T. Ziman and P. Lindgård, Phys. Rev. B **33**, 1976 (1986).
[23] C. R. Fincher, G. Shirane, and S. A. Werner, Phys. Rev. B **24**, 1312 (1981).
[24] G. Grüner, Rev. Mod. Phys. **66**, 1 (1994).
[25] H. Z. Cummins, Phys. Rep. **185**, 211 (1990).
[26] P. Bak, Phys. Rev. Lett. **37**, 1071 (1976).